探討具有偏極化寬譜線與不具有偏極化寬譜線之西佛二型星系

俞伯傑、黃崇源
國立中央大學天文研究所

摘要：

我們探討了具有偏極化寬譜線與不具有偏極化寬譜線之西佛二型星系的一些特性，包括近紅外、[O_{III}]發射線、核心塵埃型態與質量。我們從哈伯太空望遠鏡的影像來分析核心一千個秒差距（1 kpc）內的塵埃型態跟質量。這兩種西佛二型星系在核心塵埃型態上並沒有顯著的不同，這與之前的研究結果並不一致。而在近紅外線的比較上，這兩種西佛二型星系呈現出顯著的差異，也暗示著這兩種西佛二型星系是被不同的機制所主宰。

Investigation of Hidden Broad-line Region and Non-hidden Broad-line Region Seyfert 2 Galaxies

Yu Po-Chieh, Hwang Chorng-Yuan
Institute of Astronomy, National Central University

ABSTRACT

We investigate and compare some properties of hidden broad-line region (HBLR) Seyfert 2 and non-HBLR Seyfert 2 galaxies, including near-infrared, [O_{III}] emission nuclear dust morphology, and dust mass. We obtain optical images from Hubble Space Telescope to probe the nuclear dust structures of these galaxies within 1 kpc regions and dust masses inside the 1 kpc regions (M_{1kpc}) are estimated from obscuration levels. Dust morphology shows no significant difference between HBLR and non-HBLR Seyfert 2 galaxies, this is significantly in contrast to the results of previous studies. We also compare the dust obscuration levels in host galaxies of HBLR and non-HBLR Sy2s using some properties, such as nuclear dust mass and mass ratio M_{1kpc}/M_{Total}. At last, we compare the near-infrared colors of HBLR and non-HBLR Seyfert 2 galaxies and the results show that they are dominated by different mechanisms.

關鍵字（Key words）：星系（Galaxies）：活躍（Active）、星系核（Nuclei）、西佛（Seyfert）

1. Introduction

Active galactic nuclei (AGNs) are very powerful phenomena in the universe. Several types of AGNs have been found, such as Seyfert galaxies, quasars, and BL Lac objects. Seyfert galaxies are divided into two subtypes: Seyfert 1 (Sy1) and Seyfert 2 (Sy2), according to their different optical line widths. The discovery of polarized broad emission lines in NGC 1068 suggested that Sy2s were the same object as Sy1s but viewed from a different orientation (Antonucci & Miller, 1985; Antonucci 1993). However, previous studies showed that only about 40 - 45% of Sy2s show polarized hidden broad line region (HBLR) (Gu & Huang, 2002; Heisler et al., 1997). This result is not consistent with the standard unification model. It is unclear why only some Sy2s have detectable HBLRs. There were several explanations; however, none conclusive results have been obtained. Some properties of HBLR and non-HBLR Sy2s have been investigated, such as radio, far infrared, and X-ray emission. These previous studies suggested that the HBLR and non-HBLR might be intrinsically different populations. In many respects, the HBLR Sy2 is similar to a Sy1, suggesting that the HBLR Sy2s do harbor a central AGN, such as X-ray lumi nosity, spectral hardness, and spectral cutoff distribution (Gu & Huang, 2002; Deluit, 2004).

Nuclear spiral structures are expected to trace possible mechanisms for fueling AGNs (Fukuda et al., 1998; Montenegro et al., 1999). Based on the Hubble Space Telescope (HST) snapshot imaging survey of Seyfert galaxies (Malkan et al., 1998), Gu et al. (2001) found that none of the HBLR Sy2s show dust lanes crossing the nucleus while about 30% of non-HBLR Sy2s show such dusty nuclear structures. They suggested that the polarized broad lines are hidden by obscuration crossing the nuclear regions. Based on the same imaging survey, Tran (2003) found that the fraction of the non-HBLR Sy2s that show dust lanes is 10/18 (55%), while the corresponding fraction for the HBLR Sy2s is only 3/11 (27%), which is similar to that for Sy1s (23%). These results suggested that circumnuclear dust morphology of the host galaxies might have a significant influence on the origin of the non-HBLR and HBLR Sy2s. In this paper, we investigate the circumnuclear dust morphology for a sample of HBLR and non-HBLR Seyfert 2 galaxies using optical images obtained from the HST archive. These images are fitted with the Galfit package (Peng et al., 2002) to probe the inner structures of these galaxies within the central 1 kpc regions. We discuss the difference and similarity between these two types of Sy2s based on their dust morphology and derived dust masses. We also compare some other observed properties, such as [O_{III}], and near-infrared emission.

2. Sample and Data Reduction

We have selected high-resolution images for a sample from the HST archive to investigate the nuclear regions of HBLR and non-HBLR Seyfert 2 galaxies. Most of the selected sources have been observed by Tran (2003) using telescopes at the Lick and Palomar observations. There are a total

of 30 sources in our selected sample: 14 are HBLR Seyfert 2 galaxies and 16 are non-HBLR Seyfert 2 galaxies. All images were taken with the F606W filter (central wavelength: 5957 Å), except Mrk 573 (F569W, central wavelength: 5623 Å) and NGC 5283 (F702W, central wavelength: 6895 Å).

We reduced the HST archive images following standard data reduction procedures. We first removed the cosmic-ray hits in the images by using the COSMICRAYS task in the NOAO IRAF package, then fitted each image with a galaxy model with the Galfit package (Peng et al., 2002). An exponential disk, a Sérsic profile, and a Gaussian function have been included in our fitting. The nuclear structures of these galaxies are obtained after subtracting the fitted models from the observed images. In Figure 1 we show the images of NGC 6890 as an example.

Dust masses in the central regions of these galaxies are estimated from the residual images. We follow van Dokkum & Franx (1995) to estimate the mass of the dust present in each residual image. The dust mass is given by $M_{dust}(M_\odot)=A_v \Sigma \Gamma^{-1}$, where A_v is the mean visual extinction in magnitudes, Σ is the surface area covered by the dust, and Γ is the extinction coefficient per unit mass. We adopt $\Gamma=6\times10^{-6}$ mag kpc^2 $M^{-1}_\odot$ (van Dokkum & Franx 1995). The mean visual extinction A_v is related to the optical depth τ by $A_v=1.0857\,\tau$, and the optical depth is obtained by comparing the observed and model fluxes with $\tau=\ln(F_{obs}/F_{model})$. We first calculate the optical depth for each pixel to get the mass Δm per pixel size and then sum over the Δm in the central 1 kpc region to get the total central dust mass.

3. Result and Discussion

3.1 Circumnuclear Dust Morphology

The dust morphology of HBLR and non-HBLR Sy2s are classified into three different classes following Martini et al. (2003) to compare the nuclear dust structures. The galaxies that show nuclear spiral dust structures, including multiarm spirals, symmetric, two-arm spirals, and one-arm spirals, are all classified as S class. The galaxies that show chaotic morphology are classified as C class. The galaxies that have no obvious nuclear dust structures are classified as N class. In Figure 2 we show these classes of dust morphology, and in Figure 3 we show the distributions of these different classes for both HBLR and non-HBLR

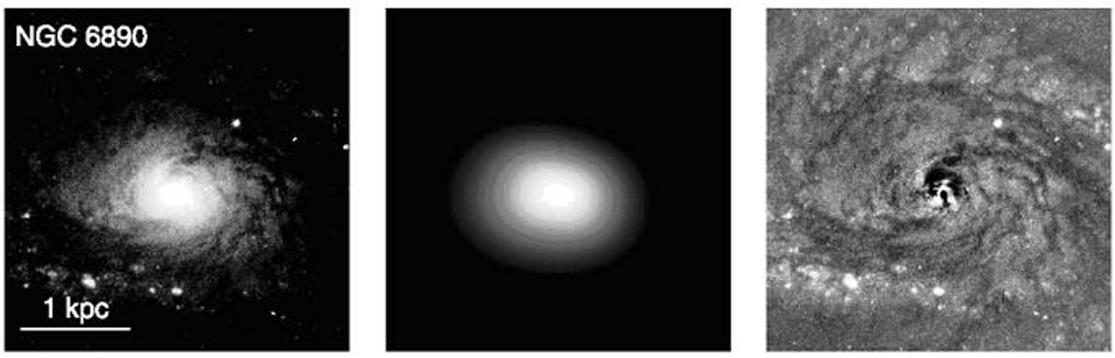

Fig. 1: Example of image fitting with the Galfit package. Left: HST image of NGC 6890. Middle: Galfit model. Right: Residual image.

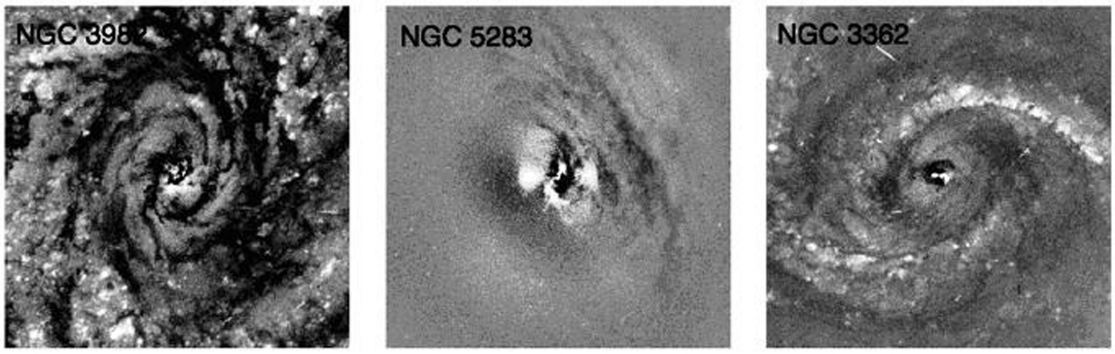

Fig. 2: Classification of dust structures in the inner region of Seyfert 2 galaxies. Left, S class; middle, C class; right, N class.

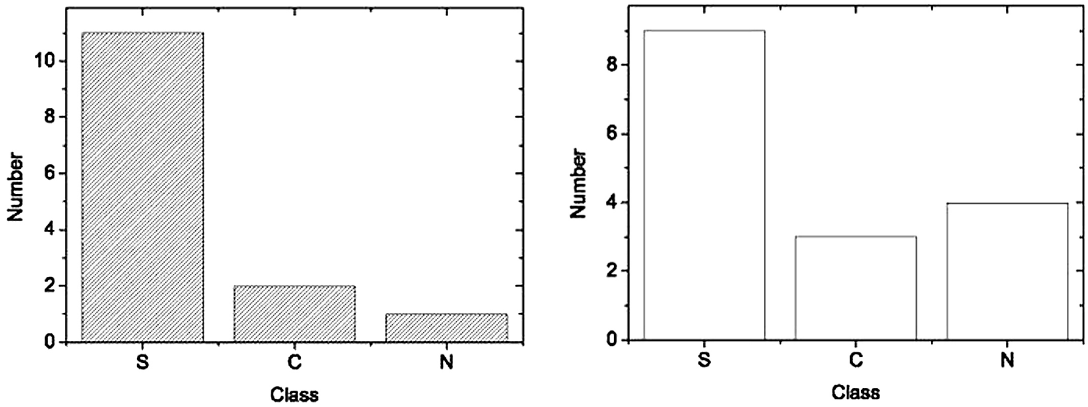

Fig. 3: Structure distributions of HBLR and non-HBLR Seyfert 2 galaxies. The HBLR and non-HBLR Seyfert 2 galaxies are shown as shaded and unshaded histograms, respectively.

Sy2s in our sample. We find that most of these Sy2s show obvious dust structures. The fractions of galaxies that show dust structures are about 92% (13/14) for the HBLR and 75% (12/16) for the non-HBLR Sy2s. This result indicates that the HBLR Sy2s possess slightly more nuclear dust structures than the non-HBLR Sy2s do; however, the discrepancy is not significant. It seems that there is no clear difference of nuclear dust structures between these HBLR and non-HBLR Seyfert 2 galaxies. This is significantly in contrast to the results of previous studies by Tran (2003).

3.2 Dust Mass

The dust mass within the central 1 kpc region have been estimated for both HBLR and non-HBLR Sy2s in our sample. The dust masses within the central 1 kpc region are around $10^{3.5}$–$10^{4.5}$ $M_{\odot}$. Figure 4 shows the dust mass distributions for the HBLR and non-HBLR Sy2s. The Kolmogorov-Smirnov (K-S) test of these two distributions shows P=15%, indicating that the distributions of the central dust masses are indistinguishable between these two types of Sy2s. We also use the T-test to test whether the means of dust mass distributions for HBLR and non-HBLR Sy2s are significantly different. The T-test result is -0.84 with a significance of 0.41, indicating that the HBLR and non-HBLR Sy2s have indistinguishable average dust masses. Therefore, we suggest that the dust obscuration levels are similar in the host galaxies of the HBLR and non- HBLR Sy2s. We note that the absorbing hydrogen column densities derived

from hard X-ray observations for these two types of Sy2s were also statistically similar (Alexander, 2001).

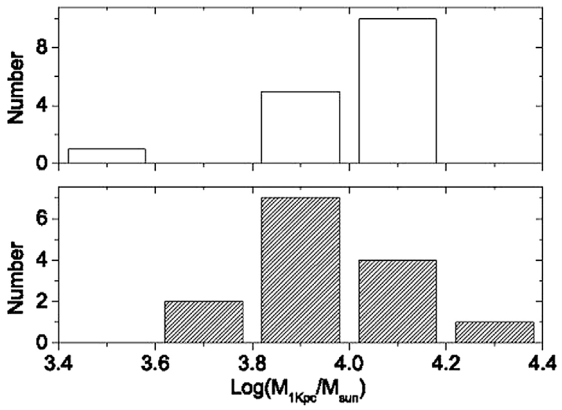

Fig. 4: Dust mass distributions of HBLR and non-HBLR Sy2s. The HBLR and non-HBLR Sy2s are shown as shaded and unshaded histograms, respectively. The K-S test of these two distributions is 0.15.

We also follow Thuan & Sauvage (1992) to derive the total dust mass of galaxies from far infrared emission. The total dust mass is given by $M_{total}(M_{\odot})=0.959\times f_{100}xD^2\times((9.96x(f_{100}/f_{60})^{1.5}-1)$, where f_{100} (Jy) and f_{60} (Jy) are flux of 100 and 60 μm respectively, D (Mpc) is the distances of the sources. Our results show that the total dust masses of galaxies are around 10^5 to 10^7 $M_{\odot}$. We compare the average mass ratio of HBLR and non-HBLR Sy2s. The average mass ratio M_{1kpc}/M_{Total} of the HBLR is 0.06, which is slightly larger than that of the non-HBLR (0.03). The mass ratio M_{1kpc}/M_{Total} shows that the dust mass distributions of HBLR and no-HBLR Sy2s are similar. Again, this result suggests that HBLR and non-HBLR Sy2s could have very similar dust obscuration levels in their host galaxies.

For the bugles of spiral galaxies and large elliptical galaxies, the distribution of surface brightness typically follows the $r^{1/4}$ law (also called Sérsic function.). And the exponential disks are used for the disk of spiral galaxies. The physical reasons why the surface brightness follows the Sérsic function and the exponential disk are still unknown. There could be some clues of galaxy formation by investigating the relation of dust mass within nuclear regions and the length scales. We can get length scales of Sérsic component (R_s) and exponential disk (R_e) respectively from fitted parameters. Figure 5 shows that there is no significant R_s/M_{1kpc} and R_e/M_{1kpc} correlations for HBLR and non-HBLR Sy2s. The correlation coefficients of R_s/M_{1kpc} are 0.05 ($P=85\%$) and -0.17 ($P=53\%$) for HBLR and non-HBLR Sy2s respectively. And the correlation coefficients of R_e/M_{1kpc} are 0.14 ($P=66\%$) and

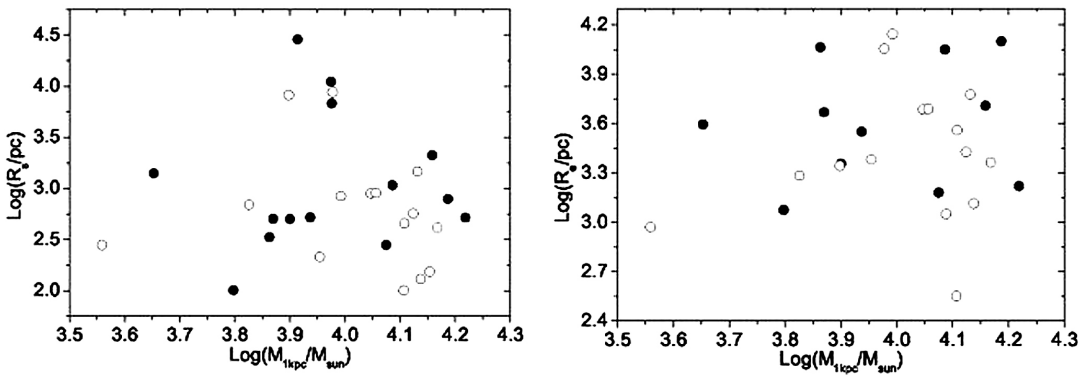

Fig. 5:The HBLR and non-HBLR Sy2s are shown as solid and open circles respectively. The correlation coefficients of R_s/M_{1kpc} are 0.05 (P = 85%) and −0.17 (P = 53%) for HBLR and non-HBLR. And the correlation coefficients of R_e/M_{1kpc} are 0.14 (P = 66%) and 0.13 (P = 63%) for HBLR and non-HBLR.

0.13 (*P=63%*) for HBLR and non-HBLR Sy2s respectively.

3.3 Near Infrared Color

Many properties of HBLR Sy2s have been compared to those of non-HBLR Sy2s, such as hard X-ray, the ratios $S_{20\ cm}/f_{60}$ and f_{25}/f_{60}. Some previous studies suggested that the HBLR Sy2s are different from non-HBLR Sy2s. But the near infrared colors have not been investigated yet. So here we present the near infrared color of HBLR and non-HBLR Sy2s to see how different they are. We obtained the Two Micron All Sky Survey (2MASS) J, H and K magnitudes of our sample from the NASA/ IPAC Extragalactic Database (NED). We apply some static methods, such K-S, T and F test, to compare the H－K colors for four kinds of galaxies (Sy1s, HBLR, non-HBLR Sy2s and HLS* galaxies). Table 1 shows all results of different tests and Figure 6 shows the near infrared color distribution.

The K-S test is used to determine if two

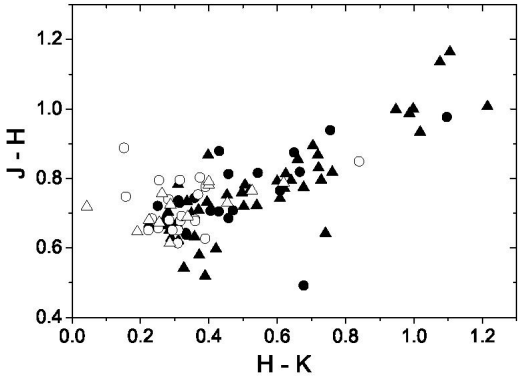

Fig. 6: The J-H and H-K color of Sy1s, HBLR, non-HBLR, and HLS galaxies. The HBLR and non-HBLR Sy2s are shown as solid and open circles respectively. The Sy1s and HLS galaxies are shown as solid and open triangles respectively. The tests shows that the near infrared color of HBLR is similar to Sy1s while non-HBLR Sy2s is more like HLS galaxies.

Table 1: The results of three static tests for Sy1s, HBLR, non-HBLR and HLS galaxies. The Sy1s and HBLR Sy2s are indistinguishable in H－K colors. The tests also show that the H－K colors of HBLR and non-HBLR Sy2s are very different.

	K-S Test	T-test	F-Test
Sy1s vs. HBLR Sy2s	P = 27.6%	P = 82%	P = 70%
HBLR vs. non-HBLR	P = 0.2%	P = 98%	P = 99.9%
Non-HBLR Sy2s vs. HLS	P = 26.1%	P = 36%	P = 45%

datasets are different significantly. The K-S test of Sy1s and HBLR Sy2s shows *P*=27.6, indicating that the distribution of H－K colors are indistinguishable between Sy1s and HBLR Sy2s. And the distribution of H－K colors are different significantly between HBLR and non-HBLR Sy2s while they are indistinguishable between non-HBLR Sy2s and HLS. These results show that the HBLR Sy2s are similar to Sy1s while non-HBLR Sy2s are more like HLS galaxies. We also use the T-test to see whether the H－K colors of the HBLR and non-HBLR Sy2s have significantly different means. And we use F-test to see if the H－K colors of the HBLR and non-HBLR Sy2s have significantly different variances. The results of T-test and F-test also show similar results of K-S test. The near infrared colors are dominated by stellar populations and represent the environments of host galaxies. Our results indicate that the HBLR Sy2s could have very different global properties of host galaxies. However, Gu & Huang (2002) found that the statistical medians of morphological type distributions are Sa and Sab for both HBLR and non-HBLR Sy2s. This result shows that the HBLR and non-HBLR Sy2s are not significantly different. Our results suggest that there might be different operative mechanisms for the near-infrared emission of these two types of Sy2s. One possibility is that HBLR Sy2s harbor a central AGN, while non-HBLR Sy2s do not. Then

* HLS: H Ⅱ, LINER and starburst galaxies.

the near infrared emission of HBLR Sy2s could be affected by the central AGN. Therefore, the HBLR Sy2s show similar near infrared color to Sy1s while non-HBLR are like HLS galaxies.

3.4 [O III] Emission

The [O_{III}] strength is a measure of AGN activities. Previous studies showed that the [O_{III}] luminosities ($L_{[OIII]}$) of HBLR Sy2s were more powerful than those of non-HBLR Sy2s (Tran2003). They also showed that the distributions of $L_{[OIII]}$ for both HBLR Sy2s and Sy1s are similar to each other, but different from that of non-HBLR Sy2s. However, the unification model predicts that an isotropic property, such as $L_{[OIII]}$, should be the same between Sy1s and Sy2s, and only galactic properties, such as dust in the galaxies, might affect the[O_{III}] strength. Figure 7 shows that there is no significant correlation between M_{1kpc} and $L_{[OIII]}$. This result indicates that the dust obscuration of host galaxies is not responsible for the difference of the $L_{[OIII]}$ between the HBLR and non-HBLR Sy2s. However, we find that there is a strong correlation between the [O_{III}] strengths and the redshift (Figure 7). The [O_{III}]/redshift correlation coefficient are 0.49 (P=98.6%) and 0.42 (P=94.4%) for HBLR and non-HBLR Sy2s respectively. This result indicates that there might be some selection bias in detecting the [O_{III}] emission of the Sy2s. So we must be careful in interpreting the previous result that the $L_{[OIII]}$ of HBLR Sy2s were more powerful than those of non-HBLR Sy2s.

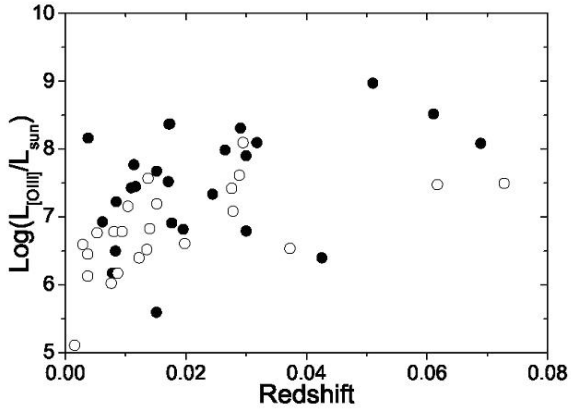

Fig. 7: [O_{III}] luminosity versus the redshift for HBLR and non-HBLR Sy2s. The correlation coefficient R is 0.49 for HBLR Sy2s and 0.42 for non-HBLR Sy2s. The result shows that the [O_{III}] strengths correlate with redshift for both HBLR and non-HBLR Sy2s.

4. Conclusion

The nuclear dust properties of HBLR and non-HBLR Sy2s have been investigated by fitting the HST images with the Galfit package. There is no clear difference of nuclear dust structures between these HBLR and non-HBLR Sy2s. This result is significantly in contrast to the results of previous optical studies. The HBLR and non-HBLR Seyfert 2 galaxies also have indistinguishable average dust masses and dust mass ratio (M_{1kpc}/M_{total}), suggesting that the dust obscuration levels are similar in the host galaxies of these two types of Sy2s. On the other hand, we find that there are significant differences in the H－K colors between the HBLR and non-HBLR Sy2s. These results indicate that there are different operative mechanisms of the HBLR and non-HBLRSy2s. However, the [O_{III}]/redshift correlation indicate that there could be some selection bias in detecting the [O_{III}] emission of the Sy2s. We must be careful in interpreting the previous result that the $L_{[OIII]}$ of HBLR Sy2s were more powerful than those of non-HBLR Sy2s.

Acknowledgement

We thank Chien Y. Peng for help and providing the Galfit program. We thank Chung-Ming Ko, Ping-Hung Kuo and Yi-Wen Cheng for useful discussions and suggestions. We also want to thank Zhi-Wei Zhang and An-Chen Chen for helping with image data processing. This work was partially supported by the National Science Council of Taiwan (grant NSC 94-2112-M-008-019). Some of the data presented in this paper were obtained from the Multimission Archive at the Space Telescope Science Institute (MAST). STScI is operated by the Association of Universities for Research in Astronomy, Inc., under NASA contract NAS5-26555. This research has made use of the NASA/IPAC Extragalactic Database (NED), which is operated by the Jet Propulsion Laboratory, California Institute of Technology, under contract with the National Aeronautics and Space Administration.

REFERENCES

Alexander, D. M. 2001, *MNRAS*, 320, L15

Antonucci, R. R. J. 1993, *ARA&A*, 31, 473

Antonucci, R. R. J., & Miller, J. S. 1985, *ApJ*, 297, 621

Deluit, S. J. 2004, *A&A*, 415, 39

Fukuda, H., Wada, K., & Habe, A. 1998, *MNRAS*, 295, 463

Gu, Q., Maiolino, R., & Dultzin-Hacyan, D. 2001, *A&A*, 366, 765

Gu, Q., & Huang, J. 2002, *ApJ*, 579, 205

Heisler, C. A., Lumsden, S. L., & Bailey, J. A. 1997, *Nature*, 385, 700

Malkan, M. A., Gorjian, V., & Tam, R. 1998, *ApJS*, 117, 25

Martini, P., Regan, M. W., Mulchaey, J. S., & Pogge, R. W. 2003, *ApJS*, 146, 353

Montenegro, L. E., Yuan, C., & Elmegreen, B. G. 1999, *ApJ*, 520, 592

Peng, C.-Y., Ho, L. C., Impey, C. D., & Rix, H.-W. 2002, *AJ*, 124, 266

Thuan, T.X. & Sauvage, M., 1992, *A&AS*, 92, 749

Tran, H. D. 2003, *ApJ*, 583, 632

van Dokkum, P. G., & Franx, M. 1995, *AJ*, 110, 2027